Atomic scale characterization of SiO_2/4H-SiC interfaces in MOSFETs devices

A.M. Beltrán[a,b,*], S. Duguay[c], C. Strenger[d], A.J. Bauer[d], F. Cristiano[b], S. Schamm-Chardon[a]

[a]CEMES-CNRS, Univ. de Toulouse, nMat group, BP 94347, 31055 Toulouse Cedex 4, France

[b]LAAS-CNRS, Univ. de Toulouse, 7 av. du Col. Roche, 31077 Toulouse Cedex 4, France

[c]Groupe de Physique des Matériaux, UMR CNRS 6634, Université et INSA de Rouen, 76801 St-Etienne du Rouvray, France.

[d]Fraunhofer IISB, Schottkystrasse 10, 91058 Erlangen, Germany

Corresponding author: ana.beltran@icmse.csic.es

Abstract. The breakthrough of 4H-SiC MOSFETs is stemmed mainly due to the mobility degradation in their channel in spite of the good physical intrinsic material properties. Here, two different n-channel 4H-SiC MOSFETs are characterized in order to analyze the elemental composition at the SiC/SiO_2 interface and its relationship to their electrical properties. Elemental distribution analyses performed by EELS reveal the existence of a transition layer between the SiC and the SiO_2 regions of the same width for both MOSFETs despite a factor of nearly two between their electron mobility. Additional 3D compositional mapping by atom probe tomography corroborates these results, particularly the absence of an anomalous carbon distribution around the SiC/SiO_2 interface.

* Present address: Instituto de Ciencia de Materiales de Sevilla (ICMS), CSIC-Univ. Sevilla. Americo Vespucio 49 Isla de la Cartuja, 41092 Seville, Spain

Introduction

SiC is extensively studied for its potential use in power electronic devices. Its wide bandgap, high thermal conductivity and large critical electric field are advantageous properties compared to Si. Furthermore, SiC easily forms SiO_2 by thermal oxidation, enabling a simple integration in the Si technology. Among the different polytypes, 4H-SiC is the most attractive due to its largest band-gap at room temperature, high electron bulk mobility and availability.

Nevertheless, the development of metal oxide semiconductor field effect transistors (MOSFETs) based on 4H-SiC is limited because of the mobility degradation in the inversion layer [1,2]. This degradation was related to electrically active defects at the SiC/SiO_2 interface, such as C clusters [3,4] and/or changes in the C/Si ratio across the SiC/SiO_2 interface. They were observed by different transmission and scanning transmission electron microscopy (TEM and STEM, respectively) techniques, such as high resolution transmission electron microscopy (HRTEM), Z-contrast imaging [5,6] and Electron Energy Loss Spectroscopy (EELS) [7]. On the other hand, these compositional variations were not observed in later works. In fact, more recent works report that the low mobility is related to the roughness at the interface [8,9]. Note that the SiC/SiO_2 fabrication methods (substrate, post-implantation annealing, oxide growth method, post-annealing ambient) vary in all these studies.

In this work we analyze two n-channel MOSFETs manufactured on two different 4H-SiC layers. The presence of N is expected to increase the mobility results. This work tries to correlate the electron mobility with the structure and compositional distribution at the SiC/SiO_2 interface of these MOSFETs.

Experimental

Two substrates namely p-type epitaxial (p-epi) and n-type epitaxial p-implanted substrates (p-impl) were used to fabricate the MOSFETs. The objective is, depending on the substrate type, to evidence if chemical modifications exist at the SiC/SiO_2 interface that may explain the observed mobility reduction in those MOSFETs [10]. Structural and compositional distributions across the interface were performed by coupling HRTEM and spatially resolved EELS. Beside, Atom Probe Tomography (APT), a technique enabling the characterization in 3D at the atomic scale [11,12] was used to give complementary information about these SiC/SiO_2 interfaces with atomic resolution.

Both n-MOSFETs were fabricated on type 4°-off 4H-SiC (0001) Si-face epilayers: (i) p-epi is a p-type epi-layer with a net acceptor concentration of 5×10^{17} cm^{-3}, and (ii) p-impl, on an implanted n-type substrate. For the p-impl substrate, multiple aluminum implantations (at 35, 70, 140 and 300 keV) were used to form a p-type box profile with a peak concentration of 3.5×10^{17} cm^{-3}. In this last case, the net donor concentration of the n-type epilayer (nitrogen) was 3×10^{15} cm^{-3}. The substrates were provided by CREE Inc. The gate oxides of the two sets of samples were grown by an oxidation in N_2O atmosphere at 1553 K and subsequently annealed at the same temperature for 30 min under N_2 ambient. Further fabrications details and the schematic cross-section of the MOSFETs are in [10].

The channel electron mobility was determined for both MOSFET from the respective transfer characteristics. During the measurements the drain source voltage (V_{DS}) was kept constant at 100 mV to ensure that the MOSFETs are operated in the linear region. In this region, the channel acts as a resistor wherein the drain current (I_D) is proportional to V_{DS} [13]. For this case only, the field-effect mobility (μ_{FE}) for electrons in the MOSFET channel may be extracted from the collected I_D-V_G characteristics [14].

Cross-sectional TEM (XTEM) samples have been prepared by focused ion beam (FIB). The MOSFETs channel was cut along the 4H-SiC [$\bar{1}100$] direction in order to avoid the

overlapping, due to the inclination of the [0001] growth direction of the epitaxial 4H-SiC towards the $<11\bar{2}0>$ direction by 4°. HRTEM and EELS analyses have been performed with a field emission transmission electron microscope, FEI Tecnai™ F20 microscope operating at 200 kV. It is equipped with an objective lens corrected for spherical aberration dedicated for the direct observation of atomic structures at interfaces with substantially reduced contrast delocalization in the images. For local EELS studies, the microscope is also equipped with a scanning stage (STEM) allowing a focused one-nanometer sized probe and with an imaging filter (Gatan GIF TRIDIEM) used as a spectrometer. Line EEL spectrum, encompassing ionization edges of elements of interest (Si, C, O), was collected at each focused point, with a collection angle of 14.7 mrad and 7 mrad of convergence angle. The energy resolution is 1.5 eV and the real step size is below 0.5 nm. Dwell–time over 16µs ensures accurate acquisition. No binning is used. The relative compositions were extracted from a classical quantitative analysis of the corresponding ionization edges, using background window over 50eV, and plotted as a function of the distance. Normalized C/Si and O/Si ratio have been also plotted in order to minimize the effect of thickness variations on the EEL spectra. This is particularly true at the 4H-SiC/SiO_2 interface since SiC is harder than SiO_2 and a thickness gradient of ~ 30 % is usually measured at the interface.

APT samples have to be prepared in a tip-shape with an end-radius below 50 nm using standard lift-out procedures followed by an annular milling. This was made in a ZEISS dual beam NVISION40. The main preparation difficulty was related to the hardness of the SiC material. The lower sputtering rate of SiC, as compared to Si and SiO_2 ones resulted in a larger tip radius around the SiC/SiO_2 interface. Once the tip sample is prepared, it is subjected to a high potential inducing a very intense electric field at the apex of the tip. Atoms at the extremity of the tip are then field evaporated and collected one by one on a 2D position sensitive detector, enabling then a 3D reconstruction. The APT investigations were

performed using a CAMECA LAWATAP instrument with an amplified ytterbium-doped laser at a wavelength of 343 nm with an energy of 25 nJ/pulse, a 350 fs pulse duration, spot size of 0.3 mm, and 100 kHz repetition rate. A very high probability of tip fracture during evaporation at the poly-Si/SiO_2 interface was observed due to the fact that SiO_2 and SiC phases have a very high field of evaporation as compared to Si. In order to avoid tip fracture, the tip was milled almost until no poly-silicon (gate material) was left on top of the tip. Although it made the APT analysis feasible, the field of view of the analysis was limited to around 20 nm due to the low thickness of the SiO_2 layer (30 nm).

Results and discussion

The field-effect mobilities for the two MOSFETs were calculated. From these μ_{FE}-V_G characteristics, the field-effect mobility of p-impl MOSFET exhibits a peak at 11.0 $cm^2V^{-1}s^{-1}$. This is about 85 % higher as compared to the one of the p-epi MOSFET field-effect mobility maximum (5.95 $cm^2V^{-1}s^{-1}$) [SI-1].

To understand this difference in mobility, samples were firstly analyzed using HRTEM (Fig. 1a and 1b). They demonstrate the good structural quality in the vicinity of the SiC/SiO_2 interface and transition between SiC and SiO_2 is clearly defined, even the steps due to the 4° off-axis of the epitaxial 4H-SiC are observed which induce a roughness at the nanometric level similar for both samples. In the SiO_2 area, the contrast is typical of an amorphous material with no specific details that could be associated to C agglomerations or graphitic clusters. Crystalline defects in the SiC substrate near the interface have not been observed. Those defects associated to the implantation of source and drain located far away from the interface should not play a role in the mobility degradation.

STEM-EELS compositional analyses were also performed. Compositional curves appear identical for both MOSFETs, p-epi and p-impl, as it can be observed on the EELS ratio

profile across the 4H-SiC/SiO_2 interface along the $<\bar{1}100>$ direction (Fig. 1c and 1d, respectively). C/Si and O/Si ratio profiles are rather constant within the SiC substrate and the SiO_2 (left and right side, respectively in Fig. 1c and 1d). Going from SiC to SiO_2 across the interface, the C/Si (O/Si) ratio decreases (increases) gradually without any observable enrichment in any of the elements. In particular, no C-rich area is detected in the SiC or in the bulk SiO_2 as it was previously reported [3-7]. From these profiles, a region of continuously varying composition including the three elements (Si, C and O) named transition layer (TL) can be defined (regions between the dotted lines in Fig. 1c and 1d). The TL is determined as the area where the slope changes due to the non-uniform composition. Several EELS profile acquired across the SiC/SiO_2 interface over the two MOSFETs reveal a similar width of the TL i.e. 2±1 nm, for measured performed with a probe size of 1 nm. Therefore, the different field-effect mobility of both MOSFETs seems not be directly related to a different stoichiometric state at the interface. However, some theoretical studies discuss the possibility of formation of carbon excess at the interface as graphite-like cluster with a size below 2 nm, which could be responsible for the high density of interface states, particularly deep states [15]. We could propose that when such small sized clusters existed, they would be not detected by EELS neither HRTEM images because of their dilute state within the thickness of the TEM lamella.

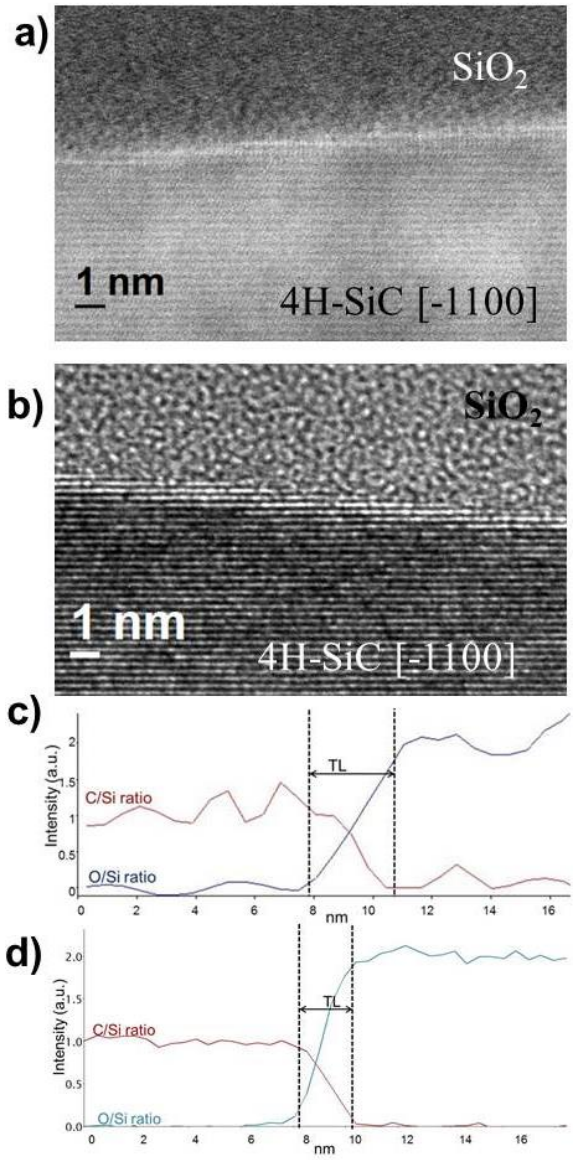

Figure 1: a) HR-STEM image of p-epi MOSFET, b) HRTEM image of p-impl MOSFET. The arrow indicates the direction of the EELS analysis. EELS ratio profiles across the 4H-SiC/SiO_2 interface for c) p-epi and d) p-impl MOSFET.

In order to investigate the presence of those sub-nanometric carbon clusters and confirm the existence of this TL layer, APT experiments have been performed. Fig. 2 shows the 3D reconstruction of the O and C elemental distributions at the SiC/SiO_2 interface for p-epi (Si is not shown as it is present in the whole analyzed area, SiO_2 and SiC). The SiC/SiO_2 interface is clearly defined for both MOSFETs, although some differences appear. As shown in Fig. 2b, in addition to the O distribution belonging to the SiO_2, O is also detected on the side of

the APT reconstruction in the SiC region. It is due to the oxidation of the SiC between the end of the FIB preparation and the introduction in the APT system.

Looking closely to the inside of the reconstruction, an oxygen-poor zone is observed at the SiC/SiO_2 interface. Concentration profiles were calculated within chosen analyzed volumes in the tip by using a sampling box of 0.3 nm width moving perpendicularly to the SiC/SiO_2 interface as shown in Fig. 2a. The region containing the surface oxidation was avoided. In the APT concentration profiles (Fig. 2b), the SiO_2 (left) and SiC areas (right) are clearly shown. In-between, a region of variable composition, which defines a TL similar to the one observed on the EELS elemental profiles. In this layer, the oxygen and carbon concentrations evolve smoothly to reach their expected values (no O in SiC and 50% of C in SiC). Looking at the Si profile, the width of this TL is limited to few nanometers. As a first conclusion from these 3D elemental distributions, it can be observed that SiC/SiO_2 interfaces are less abrupt than what it has been reported e.g. for the Si/SiO_2 interface [12]. This roughness at the interface could explain the drastic fall of mobility in the SiC substrate of these MOSFETs compared to the SiC intrinsic bulk mobility [9].

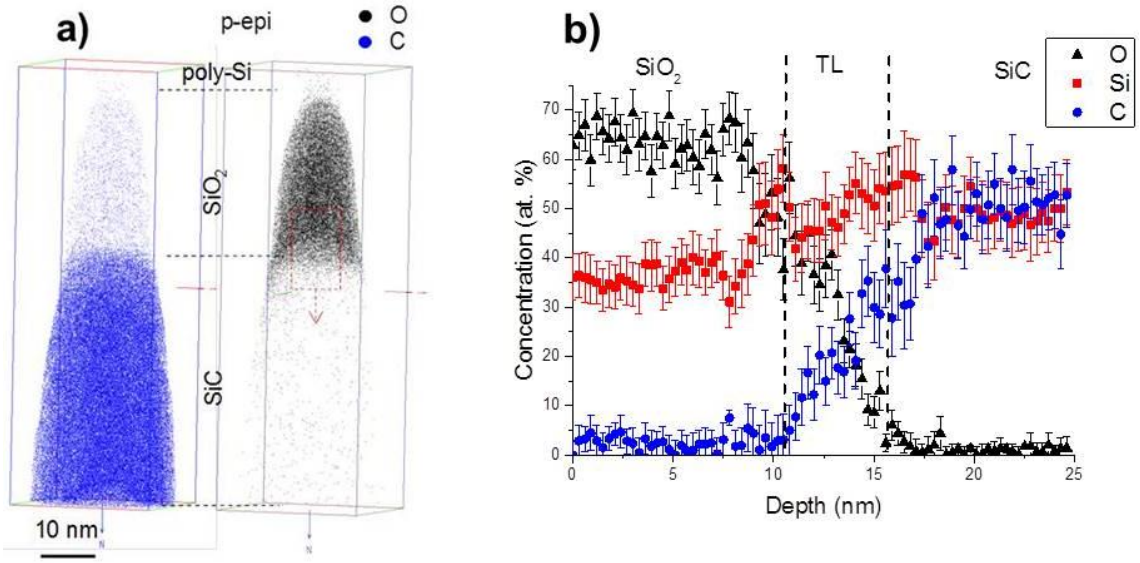

Figure 2: a) 3D reconstruction of the data from ATP analysis of the p-epi sample. b) Compositional profile plotted across the SiO_2/SiC interface as indicated by the dotted box in a.

Concerning the p-impl sample, the situation is somehow different as a local oxygen-rich inclusion is evidenced locally in the SiC region as shown in the APT reconstructions (Fig. 3a). Two concentration profiles were calculated for the p-impl sample: 1) the sampling box (5×5 nm^2 – more statistical error) was placed first outside (right arrow Fig. 3a) and then, within the oxygen inclusion (left red dashed arrow Fig. 3a). Associated concentration profiles are shown in Fig. 3b and 3c, respectively. The SiO_2 (left) and SiC areas (right) are anyway clearly shown. In-between, again a region of variable composition is observed, the TL, similar to the one observed on the EELS elemental profiles. The oxygen inclusion is clearly seen on the concentration profile (Fig. 3c) with oxygen gradually decreases across the TL layer. This O inclusion is also accompanied by a lack of C, also evidenced in the 3D reconstruction (Fig. 3a). Outside this inclusion, the situation is somehow different, a TL, associated to the C evolution, is also deduced. But the SiO_2/TL interface is measured to be very abrupt (less than 1 nm). This interface is much more abrupt than the one measured on the p-epi sample. So, on the one hand, an oxygen inclusion is observed but around a sharper interface. Hence, the larger mobility measured for the p-impl sample could be associated to this sharper interface. However, the mechanisms of the formation of this oxygen inclusion and sharper interface are unknown and some reproducibility should be confirmed by the analysis of several samples, which is not straightforward at all by APT. From this first result, it appears that C excess or C clusters presence around the SiC/SiO_2 interface is not supported either for the p-epi or for the p-impl samples. It confirms the EELS results, which were reproduced more systematically on several areas of the MOSFETs channel.

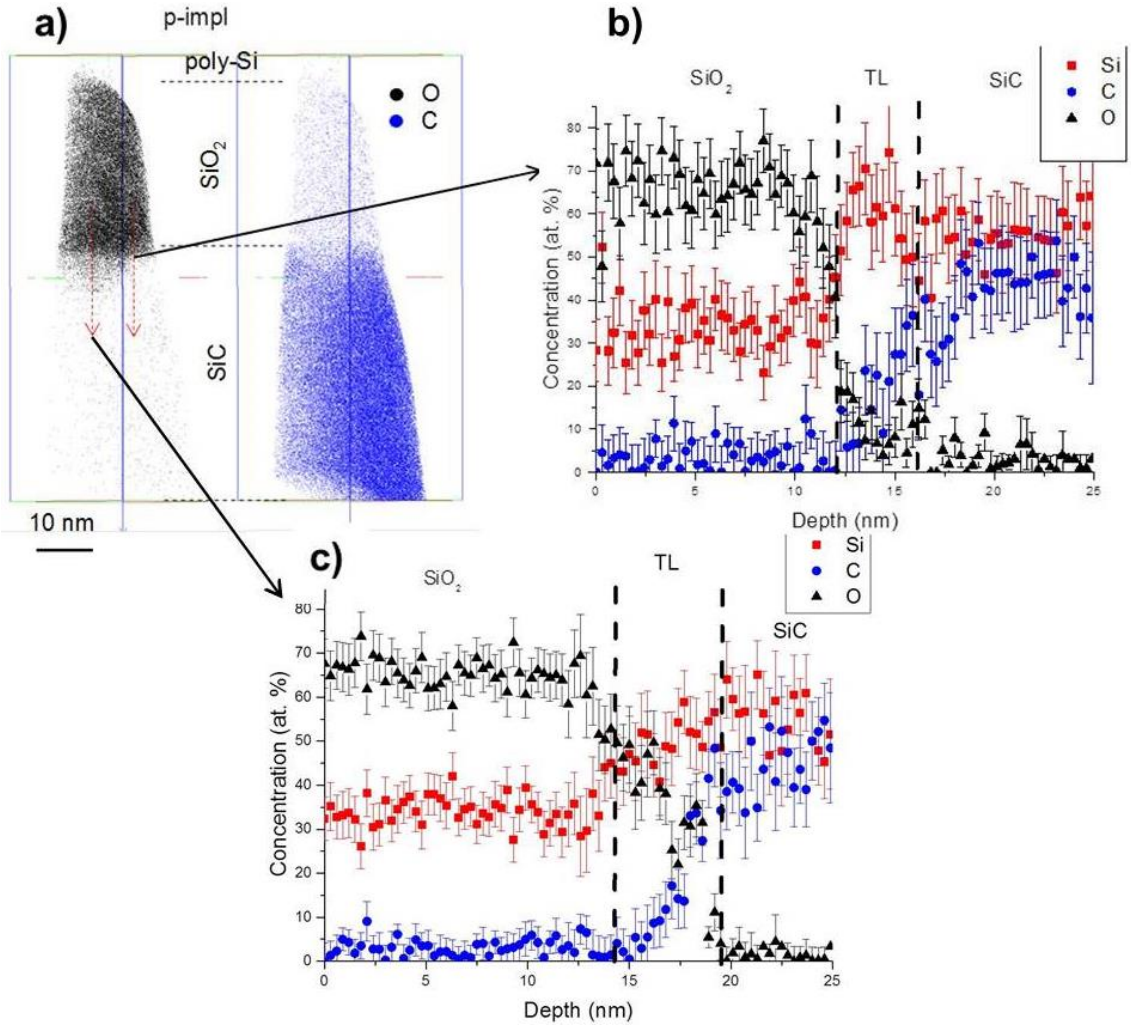

Figure 3: a) 3D reconstruction of the data from ATP analysis of the p-impl sample. Two compositional profiles were plotted across the SiO_2/SiC interface b) outside and c) within the oxygen inclusion, as indicated by dotted lines on a).

Conclusion

In conclusion, MOSFETs fabricated on p-implanted substrates present a peak field-effect mobility of MOSFET around 85% higher than those grown on p-epitaxial substrates. The novelty of this work consists in complementary elemental chemical analyses by EELS and APT. Both techniques revealed a similar compositional distribution for both MOSFETs across the dielectric/semiconductor interface. A smooth variation of the Si, C and O elemental concentrations is observed over few nanometers between the 4H-SiC substrate and the gate oxide SiO_2. No carbon excess or clusters were evidenced by both techniques. The

corresponding TL seems richer in Si and O than in C. Indeed, the surface roughness is not a limiting factor in the calculation of the mobility but its reduction contributes to the increase of the channel mobility [16]. The very local observation of a sharper interface for the p-impl compared to the p-epi sample could add an argument to explain the better mobility values measured for this MOSFET. However, the limited success of APT experiments and restricted field of view do not able to draw clear conclusions about the mobility. Improving APT tip preparation procedures could be a possible route to overcome that limitation. For example, we believe that reversing the sample, i.e. starting the APT analysis in the SiC substrate towards the SiO_2, would drastically increase the experiment success rate but also would enable a better field-of-view and then a better representation. The nature of the binding at positions around the interface will be discussed in another work based on EELS analyses of the elements edge fine structures at a sub-nanometer scale [17].

Acknowledgements

This work has been performed by the French-German Consortium MobiSiC and supported by the Programme Inter Carnot Fraunhofer (PICF) from BMBF (Grant 01SF0804) and ANR. Authors thank P. Salles and R. Cours (CEMES-CNRS) for the sample preparation by FIB. The support from Robert Bosch GmbH is highly appreciated. Authors also thanks to METSA French network for the financial support for performing APT.

Reference

[1] A. Agarwal, S. Haney, J. Elec. Mater 37 (2008) 646.

[2] S. Potbhare et al., J Appl. Phys 100 (2006) 044515.

[3] K.C. Chang et al., Appl. Phys. Lett. 77 (2000) 2186.

[4] G.Y. Chung et al., Appl. Phys. Lett. 76 (2000) 1713.

[5] T. Zheleva et al. Appl. Phys. Lett. 93 (2008) 022108.

[6] T.L. Biggerstaff et al., Appl. Phys. Lett. 95 (2009) 032108.

[7] K.C. Chang et al., J. Appl. Phys. 95 (2004) 8252.

[8] P. Fiorenza et al., J. Appl. Phys. 112 (2012) 084501.

[9] F. Roccaforte et al., Appl. Surf. Sci. 258 (2012) 8324.

[10] C. Strenger et al. Mat. Sc. Forum 717-720 (2012) 437.

[11] K. Inoue et al., Ultramicroscopy 109 (2009) 1479.

[12] M. Ngamo et al., Thin Solid Films 518 (2010) 2402.

[13] S. Sze, K. Ng, Physics of Semiconductor Devices, John Wiley & Sons, New York, 2007.

[14] D.K. Schroeder, Semiconductor Materials and device characterization, 3rd Ed. John Wiley & Sons, New York, 2006.

[15] P. Deàk et al., J. Phys. D: Appl. Phys. 40 (2007) 6242.

[16] A. Frazzetto et al., Appl. Phys. Lett. 99 (2011) 072117.

[17] Tan et al. MRS Spring Meeting 2014.